

Numerical Modeling of Impulse Waves Generated by Avalanches

Axel Giboulot
Supervised by Christophe Ancey

November 25, 2025

Contents

Contents	1
1 Introduction	2
2 Approach	2
3 Instantaneous Transformation of Snow into Water: An Equivalent Avalanche	2
4 Boundary Condition and Information Conflict	3
5 Practical Implementation: Insertion of the Equivalent Avalanche	3
6 Case Study at Trift	4
7 Limitations of the Method	4
8 Conclusion	6
References	7

Abstract

Impulse waves¹ have caused past disasters with thousands of casualties (Bosa and Petti, 2011; Mergili et al., 2020). Whereas dense flows such as landslides and icefall collapses have been responsible for such events, the drainage of Trützisee (Ammann, 2000) by an avalanche suggests that avalanches may be just as capable.

The only method available today to estimate the height of an impulse wave is an empirical relation, derived from dimensional analysis (Heller, 2008). This relation has led in practice to unrealistic predictions, and laboratory experiments have shown that it underestimates density effects (Zitti et al., 2016). Given these limitations, an alternative method is needed to estimate the height of impulse waves, particularly for avalanches.

The solution proposed here is to assume a sudden transformation of snow into water. Thus, it suffices to impose the avalanche in the tsunami model after correcting the fluxes (mass and momentum) by the density of snow. This enables the separate use of existing numerical avalanche and tsunami models.

This method has the advantage of being physically based (Saint-Venant equations) and conservative, since the energy dissipation associated with shock absorption due to snow compressibility is neglected. The wave energy is therefore limited to that of the avalanche, and the resulting waves are all the more realistic.

The case of the future Trift dam (Manso et al., 2016) is considered here, as the reservoir's exposure to avalanches makes it an ideal case study.

1 Introduction

An avalanche generates an *impulse wave* when it strikes a body of water such as a lake. This wave may damage areas near or downstream of the lake depending on its amplitude. While known historical events were triggered by dense flows such as landslides (Bosa and Petti, 2011) and icefalls (Mergili et al., 2020), the question for the Trift dam is whether avalanches can also cause large waves. More generally, we ask: how can one estimate impulse waves generated by avalanches?

2 Approach

The analytical approach to the problem is currently limited to attempts at nondimensionalization (Heller, 2008).

This option is rejected here because the effect of snow's low density is poorly captured (Zitti et al., 2016). The absence of physical limits and the ambiguity of defining the depth h_* in practical cases further motivate rejecting this approach. Numerical modeling therefore becomes advantageous and much cheaper than a physical model.

The drawback is that a single model cannot suffice, since the rheology of snow differs fundamentally from that of water. Using one model dedicated to avalanches and another dedicated to waves simplifies the equations to solve and allows using existing numerical models. To link the avalanche model to the wave model, we choose to assume an instantaneous transformation of snow into water at a certain distance from the reservoir.

Such a sudden transformation must not violate the governing equations. In practice, the Saint-Venant equations are used for both avalanches and waves. They express mass and momentum conservation. Thus, the transformation must preserve these two quantities.

3 Instantaneous Transformation of Snow into Water: An Equivalent Avalanche

The principle of Saint-Venant models is to vertically average the local mass and momentum conservation equations for an incompressible fluid and remove weakly influential terms. For each surface element dA , the unknowns are the mass $\varrho h dA$ and momentum $\varrho h u dA$ of the column. Define two avalanches \mathcal{A} and \mathcal{A}' as equivalent if their mass m and m' and momentum \mathbf{q} and \mathbf{q}' are equal everywhere. For two such avalanches

¹An impulse wave is a wave created when a flow (avalanche, landslide, or other) plunges into a body of water (such as a lake, sea, or ocean).

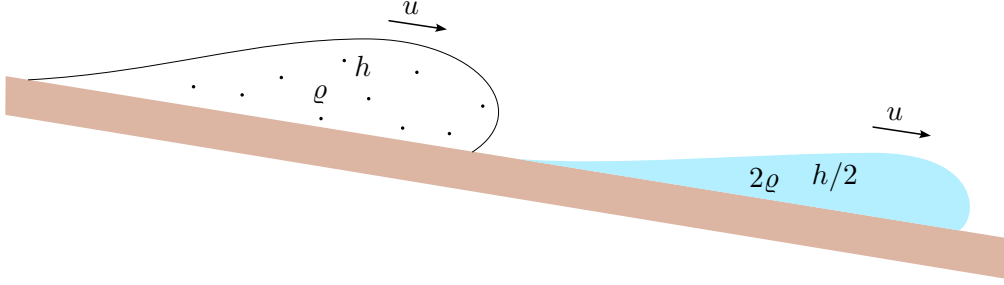


Figure 1: Two avalanches of different densities but equal mass ($m = \iint \varrho h \, dA = \iiint 2\varrho h/2 \, dA$) and momentum ($q = \iint \varrho h u \, dA = \iint 2\varrho h/2 u \, dA$).

with different densities ϱ and ϱ' , their flow depths are related by the factor $\kappa \doteq \varrho/\varrho'$. When $\varrho' = \varrho_{\text{water}}$, κ is simply the inverse relative density of avalanche \mathcal{A} .

$$\begin{aligned} \begin{pmatrix} m \\ q \end{pmatrix} &= \begin{pmatrix} m' \\ q' \end{pmatrix} \Rightarrow \begin{pmatrix} \varrho h \\ \varrho h u \end{pmatrix} = \begin{pmatrix} \varrho' h' \\ \varrho' h' u' \end{pmatrix} \\ &\Rightarrow \begin{pmatrix} h\varrho/\varrho' \\ u \end{pmatrix} = \begin{pmatrix} h' \\ u' \end{pmatrix} \end{aligned} \quad (1)$$

Thus, for avalanche \mathcal{A}' of density ϱ' to be equivalent to avalanche \mathcal{A} of density ϱ , the flow depth must be corrected by $\kappa = \varrho/\varrho'$.

The assumption of instantaneous transformation is energy-conservative: shock absorption due to snow compressibility is neglected. This assumption corresponds to an elastic impact with a restitution coefficient of 100 %.

4 Boundary Condition and Information Conflict

Once the equivalent avalanche is defined, it must be inserted correctly through boundary conditions. Typically, coupling two numerical models requires information exchange in both directions. However, flowing avalanches are usually supercritical. This means that with a *properly oriented* boundary condition, the wave model does not need to send information back to the snow model because information cannot propagate upstream. This is highly advantageous: one can simply extract results from the avalanche model and input them into the wave model without explicit coupling.

To clarify what a *properly oriented* boundary condition is, we examine the influence region of a perturbation. For first-order advection–diffusion, a perturbation propagates over δt by a translation $\mathbf{u} \delta t$ plus diffusion $\sqrt{gh} \delta t$. When flow is subcritical ($u < \sqrt{gh}$), the perturbation spreads in all directions. When supercritical ($u > \sqrt{gh}$), the perturbed region forms a cone whose angle depends on the Froude angle $\varphi \doteq \arcsin(1/\text{Fr})$, as shown in Figure 2. A conflict occurs when this perturbed region intersects the boundary. One way to avoid this risk is to impose a boundary condition that follows a contour line. Avalanches tend to follow the slope, flowing perpendicular to contour lines and therefore to the boundary, avoiding information conflicts provided the flow remains supercritical.

5 Practical Implementation: Insertion of the Equivalent Avalanche

For impulse waves caused by avalanches, the reference avalanche consists of snow (density $300 \text{ kg/m}^3 < \varrho_{\text{snow}} < 500 \text{ kg/m}^3$) and the equivalent avalanche consists of water ($\varrho_{\text{water}} = 1000 \text{ kg/m}^3$). Thus, the flow depth h_{snow} must be corrected by $\kappa = \varrho_{\text{water}}/\varrho_{\text{snow}}$ to obtain $h_{\text{water}} = \kappa h_{\text{snow}}$ according to Equation 1.

Because the rheology of snow and water differs, the distance traveled by the wave while still represented as water must be minimized so that the mass and momentum fluxes at impact match those of the snow

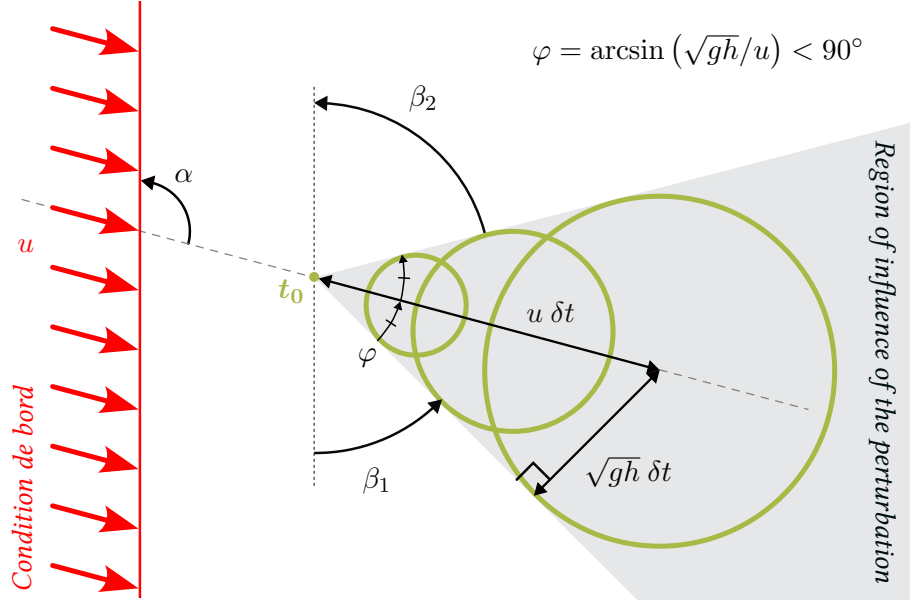


Figure 2: Propagation cone for information in a linear advection, supercritical regime. Circles show the extent of a perturbation at time $t_0 + \delta t$. The flow is supercritical while $\varphi = \arcsin(\sqrt{gh}/u) < 90^\circ$, which implies $\text{Fr} > 1$. Information conflict occurs when $\beta_1 = \pi - \alpha - \varphi < 0$ or $\beta_2 = \alpha - \varphi < 0$.

model. In other words, the boundary elevation z_b must be slightly higher than the lake level z_l by an offset $\delta z = z_b - z_l$. This offset must be sufficient to allow possible interaction between avalanche and wave.

To avoid limiting the runup² at z_b , the zones not reached by the avalanche must remain free. The boundary therefore follows the edges of the computational domain, detouring around the avalanche without descending below z_b . A summary diagram is shown in Figure 3.

6 Case Study at Trift

After more than 2 km of retreat of the Trift Glacier, a dam is planned directly downstream of the glacier (Manso et al., 2016). Located at 1767 m.s.m. and surrounded by steep slopes, the reservoir will be exposed to avalanches, making it an ideal case study to test the proposed method. An example result is shown in Figure 4, where avalanches are first simulated with AVAC³. The impulse wave reaches a maximum height of 5 m and disperses before reaching the dam.

Overflow is caused by a combination of:

- upon impacting the dam, the wave converts its kinetic energy into potential energy, greatly increasing its height, and
- wave reflections on the shores occasionally combine to form a transient, larger wave.

This second phenomenon cannot be captured by a simple analytical method because it depends directly on the two-dimensional topography.

The solution is visually satisfactory. Physically, experiments show that the peak mechanical energy of the impulse wave is about 15 % of that of the avalanche (Zitti et al., 2016; Meng and Ancey, 2019).

This relation indicates that the results obtained are realistic, whereas the empirical formula predicts a 20 m wave. Figure 5 compares the regressions of Zitti et al. (2016) and Meng and Ancey (2019) with the energies obtained.

²Runup is the upward surge of water on shorelines.

³AVAC is a GeoClaw-based code for simulating dense avalanches, available online: <https://github.com/cancey/AVAC>.

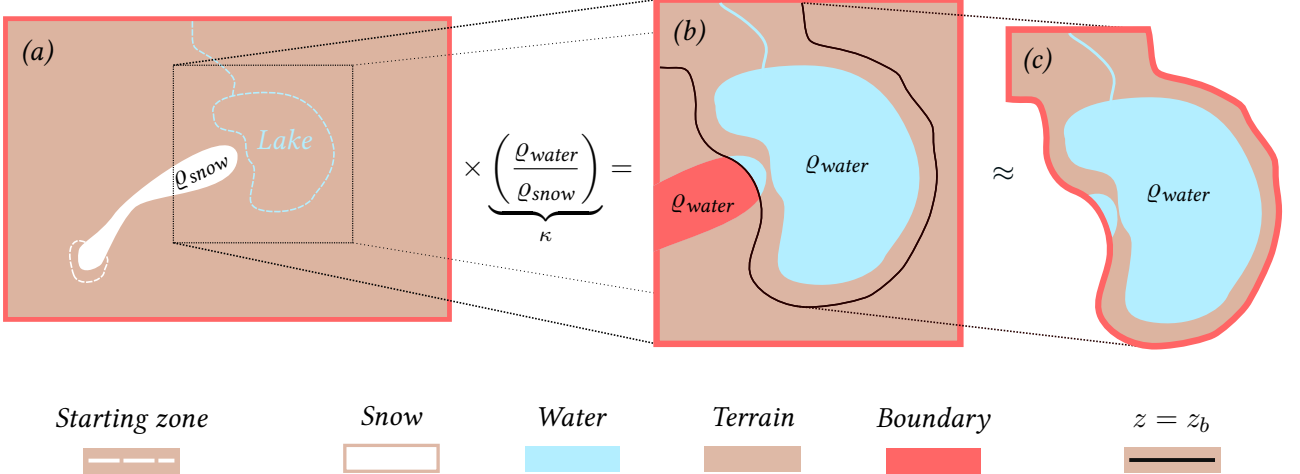


Figure 3: Simulation schematics. (a) The avalanche is first simulated with the snow model, then its quantities $(h, hu, hv)^\top$ are scaled by $\kappa = \rho_{\text{water}} / \rho_{\text{snow}}$. (b) The equivalent avalanche is then introduced into the water model above a contour line slightly higher than the lake. This line must be close to the lake level to minimize the distance the equivalent avalanche travels as water. (c) The equivalent avalanche may also be introduced through a curvilinear boundary condition (following the contour line) to lighten computations, at the cost of reducing space available for runup. An implementation of (b) with GEOCLAW is available online: <https://github.com/giboul/TrifGeoClaw>.

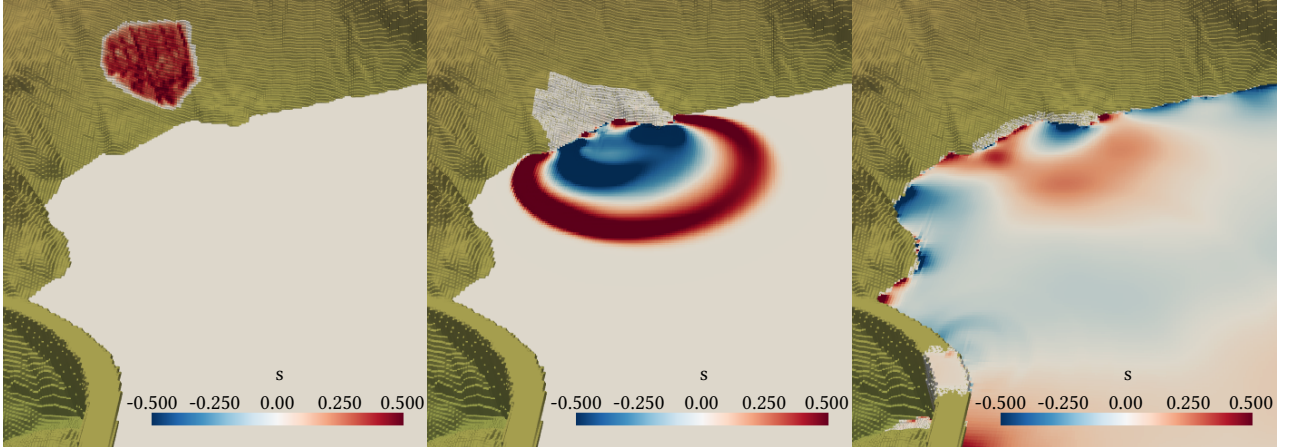


Figure 4: Simulation results of an impulse wave at Trift showing the free-surface variation $s = h - h_0$. Left: avalanche at initial time ($t = 0$), middle: impulse formation ($t = 17$ s), right: final state ($t = 1$ min 20 s).

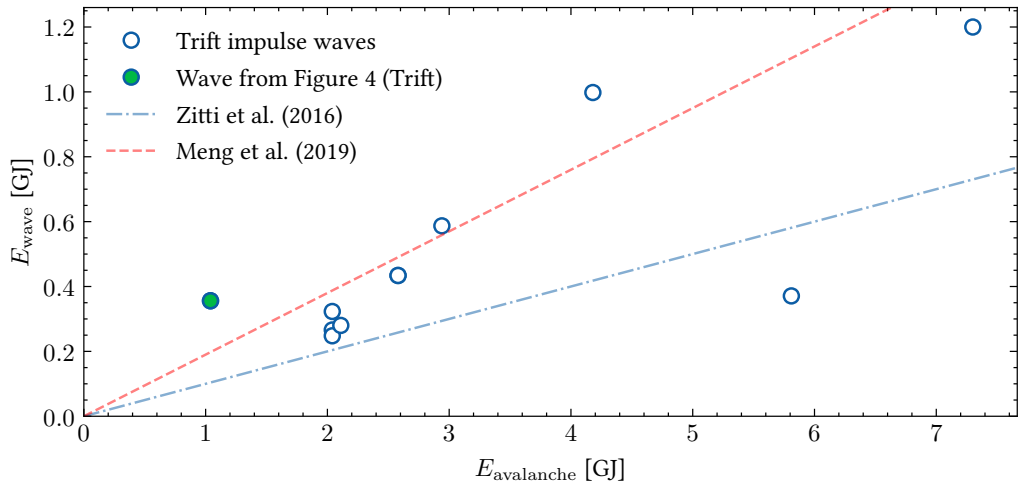


Figure 5: Ratios between mechanical energy of the wave and that of the avalanche.

7 Limitations of the Method

Here, we introduce only the mass and momentum fluxes with a density correction. The effects of more subtle quantities are not represented. For example, flow cohesion—important in wave formation—is absent (Meng and Ancey, 2019). The same applies to snow compressibility. The complexity of the snow–water mixture is also ignored because solving two-phase Saint-Venant equations is computationally expensive⁴.

8 Conclusion

Although the interaction between two phases around an impulse wave posed difficulties, the assumptions of instantaneous snow–water transformation and supercritical flow allowed us to approximate and implement the problem⁵. The proposed method makes it possible to simulate an impulse wave given a topographic survey and a prior avalanche simulation. Even if phase interaction details are neglected, the method offers a credible alternative to empirical relations.

⁴The D-Claw project (Barnhart et al., 2021) solves two-phase Saint-Venant equations.

⁵<https://github.com/giboul/TriftGeoClaw>

References

- Walter Ammann. Der lawinenwinter 1999. Technical report, Davos: Eidgenössisches Institut für Schneeund Lawinenforschung, 2000.
- Katherine R. Barnhart, Ryan P. Jones, David L. George, Jeffrey A. Coe, and Dennis M. Staley. Preliminary assessment of the wave generating potential from landslides at barry arm, prince william sound, alaska. Technical report, U.S. Geological Survey, U.S. Department of the Interior, 2021.
- Silvia Bosa and Marco Petti. Shallow water numerical model of the wave generated by the vajont landslide. *Environmental Modelling & Software*, 26(4):406–418, 2011. ISSN 1364-8152. doi: <https://doi.org/10.1016/j.envsoft.2010.10.001>. URL <https://www.sciencedirect.com/science/article/pii/S1364815210002604>.
- Valentin Heller. Landslide generated impulse waves: prediction of near field characteristics. Technical report, Versuchanstalt für Wasserbau, Hydrologie und Glaziologie, ETH Zürich., 2008.
- Pedro Manso, Anton Schleiss, Manfred Stähli, and François Avellan. Electricity supply and hydropower development in switzerland. *International Journal on Hydropower and Dams*, 23:41–47, 10 2016.
- Zhenzu Meng and Christophe Ancey. The effects of slide cohesion on impulse wave formation. *Experiments in fluids*, 2019.
- M. Mergili, S. P. Pudasaini, A. Emmer, J.-T. Fischer, A. Cochachin, and H. Frey. Reconstruction of the 1941 glof process chain at lake palcacocha (cordillera blanca, peru). *Hydrology and Earth System Sciences*, 24(1):93–114, 2020. doi: 10.5194/hess-24-93-2020. URL <https://hess.copernicus.org/articles/24/93/2020/>.
- Gianluca Zitti, Christophe Ancey, Matteo Postacchini, and Maurizio Brocchini. Impulse waves generated by snow avalanches: Momentum and energy transfer to a water body. *Journal of Geophysical Research: Earth Surface*, 121(12):2399–2423, 2016. doi: <https://doi.org/10.1002/2016JF003891>. URL <https://agupubs.onlinelibrary.wiley.com/doi/abs/10.1002/2016JF003891>.